

**$D_1 (^2B_{2g}) \rightarrow D_0 (^2A_g)$ Fluorescence From the Matrix-Isolated Perylene Cation
Following Laser Excitation into the $D_5 (^2B_{3g})$ and $D_2 (^2B_{3g})$ Electronic States.**

Xavier D.F. CHILLIER, Bradley M. STONE^a, Christine JOBLIN^b, Farid SALAMA and
Louis J. ALLAMANDOLA

Astrochemistry Laboratory, NASA/Ames Research Center, MS: 245-6, Moffett Field,
CA 94035-1000

- a. Permanent address: Department of Chemistry, San Jose State University, San Jose,
CA 95192-0101
- b. Present address: CESR-CNRS, France

Abstract: Fluorescence spectra of the perylene cation, pumped by direct laser excitation via the $D_2(^2B_{3g}) \leftarrow D_0(^2A_u)$ and $D_5(^2B_{3g}) \leftarrow D_0(^2A_u)$ transitions, are presented. Direct excitation into the D_5 or D_2 states is followed by rapid non-radiative relaxation to D_1 that, in turn, relaxes radiatively. Excitation spectroscopy across the $D_2(^2B_{3g}) \leftarrow D_0(^2A_u)$ transition near 730 nm shows that site splitting plays little or no role in determining the spectral substructure in the ion spectra. Tentative assignments for ground state vibrational frequencies are made by comparison of spectral intervals with calculated normal mode frequencies.

I. INTRODUCTION

Polycyclic aromatic hydrocarbons (PAHs), now thought to be ubiquitous throughout the interstellar medium based on their widespread infrared spectral signature¹, are also considered attractive candidates for some of the diffuse interstellar bands (DIBs), visible absorption features associated with the low density regions of interstellar space². A distribution of neutral and charged PAHs are expected to contribute to these interstellar spectra². To test the PAH-DIB hypothesis, we have developed an extensive program to measure the electronic absorption spectra of PAHs isolated in inert gas matrices^{2d-f}. Since it has recently been recognized that some DIBs are also observed in emission³, an additional test of this hypothesis requires the study of the luminescence spectra of charged, isolated PAHs. To this end, we have started a program to investigate the photoinduced luminescence of PAH cations, and have previously reported fluorescence spectra from the perylene cation^{4a} and its neutral precursor^{4b} stimulated with broadband excitation. However, while these previous studies demonstrated that the luminescence could be observed in Ne and Ar matrices, the broadband nature of the excitation source precluded detailed spectroscopic studies of the molecular physics leading to ambiguities in interpretation. To overcome this limitation, the experimental apparatus has been upgraded to include a tunable laser excitation source and a dedicated monochromator⁵. Here we report the application of this technique to the perylene cation isolated in an argon matrix.

The purpose of this study is to: (i) confirm the results of *Joblin et al.*^{4a} for the fluorescence of PAH ions, (ii) use narrow band excitation to address the questions that were raised when using a broadband excitation source concerning the role of site effects versus very low frequency modes as an explanation of the rich spectral substructure of the perylene cation above 790 nm, and (iii) discuss the implications of these experimental results for astrophysics.

II. EXPERIMENTAL

A UV/Vis/NIR spectrometer, coupled to a tunable Alexandrite laser system and closed-cycle, helium-cooled cryostat (10 K) was used to measure the electronic absorption and emission spectra of neutral or ionic species of astrophysical interest using matrix isolation spectroscopy. The apparatus consists of:

(i) The Cryogenic Sample Chamber: The sample chamber, a small cube 10 cm on a side, is part of a stainless-steel, high vacuum system. It contains four large ports (at 90° with respect to one another) and two gas injection inlets at 45° angles with respect to the ports. The cryogenic sample holder, suspended in the center of the chamber, accommodates a 20 × 1 mm sapphire window that is rotatable through 360°. A high vacuum ($p < 2 \cdot 10^{-8}$ T) was continuously maintained with a combination of diffusion and mechanical pumps. The pressure was monitored with ion and thermocouple gauges mounted on the manifold. The sapphire substrate was cooled to 10K using a closed-cycle cryostat (APD Cryogenics Inc.) and temperatures were monitored with Fe-Au/Chromel thermocouples (Scientific Instruments) separately mounted on the window holder and cryostat. The two ports along the main optical axis, equipped with quartz windows, were used to record absorption spectra. The VUV photoionizing radiation and laser excitation utilized the same port, equipped with a MgF₂ vacuum window mounted at 90° with respect to the main optical axis. The PAH deposition furnace was mounted on the fourth port.

(ii) The Optical System: Light dispersion and detection was achieved using a Czerny-Turner configured monochromator (Oriel MS 257-F_N 4.3) coupled to a 1026 x 256 pixel CCD detector (Oriel, Instaspec). The monochromator was equipped with a rotatable four-grating turret, permitting grating change without realignment. Absorption spectra from 500 to 800 nm were recorded using a 300 line/mm grating blazed at 400 nm, while the laser-induced luminescence spectra spanning the range from 750 to 1500 nm were measured with a 200 line/mm grating blazed at 1000 nm. The light from the chamber was collected and focused on the entrance slit with two fused silica glass lenses (diam.= 4 cm, f.l.= 5 cm), placed 10 cm from the sample. The typical aperture for the

entrance slit of the monochromator was set at 75 μm for absorption and 150 μm for emission measurements. The CCD detector was cooled to -10°C . The signal was integrated over 25-100 scans at a typical exposure time of 0.1 s per scan for absorption and 1 s for emission measurements. This set-up provided a typical resolution of 0.3 nm for absorption and 0.5 nm for emission

A stabilized W lamp (Oriel, model 66184, 100 W) provided the light source for the absorption measurements in the 400 to 800 nm region. An optical density filter (O.D. 1) and H_2O filter, placed between the lamp housing and sample chamber, were used to reduce the IR photon flux and prevent photobleaching of the sample.

(iii) The Laser Excitation System: An Alexandrite laser (Light Age, PAL-100), with a tunable wavelength range of 715-800 nm (fundamental) was used directly as the excitation source for pumping of the $D_2 \leftarrow D_0$ transition. Typical laser powers of 50-300 mW, at 10 Hz (long-pulse and Q -switched mode) were used. The beam was expanded by a telescope (with a magnification of x7) so that the entire sapphire window was irradiated. The excitation of the $D_3 \leftarrow D_0$ transition at 535 nm was performed as follows: the fundamental frequency ω (Q -switched mode) is first doubled with a BBO monocrystal (5x5x6 mm - in an *Inrad Autotracker III*) and gives a tunability for 2ω between 357-400 nm. This is then shifted by stimulated Raman scattering through a 1 meter Raman cell (*Light Age Inc. Raman Converter*) filled with 2500 kPa of pure hydrogen (providing a wavelength shift of 4155 cm^{-1}). The second Stokes beam ($2\omega - 8310\text{ cm}^{-1}$) was selected using a Pellin-Broca dispersion prism and sent through the telescope to the target. Sharp cut-off filters (*Corning 3-66, 3-67*) were used at times to minimize exposure of the CCD to scattered laser light.

(iv) Photoionization: The vacuum ultraviolet radiation (10.2 eV) used to ionize the sample was generated by a microwave-powered, flowing hydrogen, discharge lamp. The lamp consists of a glass discharge tube mounted in a tunable McCarroll cavity that is powered by a 50-120 W microwave generator (Ophos Instruments MPG 4M). The lamp, equipped with a removable MgF_2 window, was mounted on one port of the cryogenic chamber during photolysis. With a 10%

H₂/Helium mixture in a low pressure discharge, much of the most energetic VUV radiation is practically monochromatic in the Lyman- α line (121.6 nm).

(v) Sample Preparation: Perylene was vaporized (135^oC) under vacuum and co-deposited with Ar on the cold (10K) sapphire window. Typical argon/perylene ratios of close to 2000 were achieved in this manner. After probing the sample in absorption to check the degree of isolation of the trapped molecular species and the ionization yield, laser induced luminescence measurements were performed. For the later, the hydrogen lamp was removed, and the laser beam was directed to the sample through the MgF₂ vacuum window. The cold sapphire window was rotated to ~45^o with respect to the laser beam for the emission measurements.

III. RESULTS AND ASSIGNMENTS

The absorption spectrum of the perylene ion is presented in Fig.1. This has a somewhat lower spectral resolution than the spectrum previously reported by *Joblin et al.*^{4a} since the optical components in the system used for the results described in this paper are optimized for fluorescence rather than for absorption. Assignments for the electronic states and corresponding electronic transitions reported in Table 1 have been made based on comparisons to the photoelectron spectroscopic (PES) work of *Boschi et al.*⁶, the argon matrix absorption spectroscopic work of *Szcepanski et al.*⁷, and recent theoretical calculations by *Hirata et al.*⁸ Our previous paper^{4a} describing broad band excitation/fluorescence spectroscopy of the perylene cation based electronic assignments on the earlier theoretical calculations of *Negri and Zgierski.*⁹ There are some differences in the ordering and identification of the electronic states of the cation between this and the earlier work. These differences reflect a discrepancy in the ordering of the three lowest excited states of the perylene cation between the QCFF/PI + CI and TDDFT calculations. In particular, we note that the transition previously associated with the D_3 electronic state we now assign to D_2 following the recent work of *Hirata et al.*⁸, which shows that transitions from D_0 to D_3 are forbidden by symmetry arguments.

The strongest absorption peak (as seen in Fig. 1) is located at 535 ± 0.3 nm and is associated with the $D_5(^2B_{3g}) \leftarrow D_0(^2A_u)$ transition. The $D_2(^2B_{3g}) \leftarrow D_0(^2A_u)$ transition, observed near 730 nm, is considerably weaker and shows substructure at 728 and 733 nm as well as a few other minor features. We assign the weak band at 793 nm to the lowest energy transition $\{D_1(^2B_{2g}) \leftarrow D_0(^2A_u)\}$. This is based on the emission spectrum discussed below. The $D_4(^2B_{2g}) \leftarrow D_0(^2A_u)$ transition may be responsible for the broad absorption centered near 646 nm, just above the background. Perusal of Table 1 indicates that this transition is predicted to be stronger than that for $D_2 \leftarrow D_0$ by *Hirata et al.*⁸, but weaker by *Negri et al.*⁹

Emission corresponding to the $D_1(^2B_{2g}) \rightarrow D_0(^2A_u)$ transition for the perylene cation following direct excitation of the $D_2(^2B_{3g}) \leftarrow D_0(^2A_u)$ at 731.2 nm and the $D_5(^2B_{3g}) \leftarrow D_0(^2A_u)$ transition at 530

nm is presented in Fig. 2. The peak positions and relative intensities are very similar, regardless of the initial excitation state. In both cases, we have searched for emission directly to the red of the laser excitation position and were unable to detect any emission between the laser excitation wavelength and 792 nm (0-0 for the $D_1 \rightarrow D_0$ transition, see the next section). The absence of any emission shorter than 792 nm strongly suggests that rapid *non-radiative* relaxation to D_1 is the dominant relaxation channel for both D_2 and D_3 .

Due to the narrower bandwidth and higher intensity afforded by laser excitation, a richer emission spectrum was observed than previously reported following broadband excitation⁴. The positions of emission features observed following excitation with 731.2 nm photons (labelled and shown in Fig. 3 on a nm and cm^{-1} scale) are listed in Table 2, along with a comparison to the vibrational frequencies calculated for the 2A_u state by *Langhoff*⁴⁰. The major vibronic band separations listed in Table 2 match, within 33 cm^{-1} or less, the calculated vibrational frequencies. Assignments were made as follows:

0 \rightarrow 0 transition: The emission induced by exciting the $D_2({}^2B_{3g}) \leftarrow D_0({}^2A_u)$ band near 730 nm (Figs. 3 and 4) indicates that rapid non-radiative relaxation occurs to the D_1 state, followed by radiative relaxation $\{D_1({}^2B_{2g}) \rightarrow D_0({}^2A_u)\}$ to various vibrational levels in D_0 . Given that the 792.2 nm band is the highest energy emission band observed, this is assigned to the 0-0 transition. This assignment is consistent with that in the absorption spectrum shown in Fig.2 and assigned to the $D_1({}^2B_{2g}) \leftarrow D_0({}^2A_u)$ transition. The absorption spectrum reported by *Szczepanski et al.*⁷ contains a weak band at 791.2 nm. The theoretical value of the D_1 - D_0 transition calculated by *Hirata et al.*⁸ lies somewhat to the blue (765.3 nm, see Table 1). While the 0-0 band of the $D_1({}^2B_{2g}) \leftarrow D_0({}^2A_u)$ system (and in fact the entire system) appears weak in absorption (compared with absorption to D_3), this transition is fully allowed via the y-polarization (B_{2u}) and the 0-0 appears relatively intense in the $D_1 \rightarrow D_0$ emission spectrum (see Figs. 2, 3 and 4).

Vibrational analysis: Since calculations show that the lowest *quadruplet* (*Q*) states of PAH ions lie at higher energy than the lowest *doublet* (*D*) states¹¹, emission bands at lower energy than the 0-0 band are confidently interpreted as fluorescence (spin-allowed) transitions, rather than phosphorescence. It can be seen in Fig. 4 that the first strong band after the 0-0 band falls at 815.3 nm (labelled C_1^0 , 357 cm⁻¹ from the 0-0 position), which is close to the frequency of an a_g skeletal vibrational mode calculated at 351 cm⁻¹. The two other strong bands, those at 883 nm (H_1^0) and 906 nm (J_1^0) fall at 1298 cm⁻¹ and 1597 cm⁻¹ from 0,0. These correspond to the combined C-C stretch/C-H in - plane bending and pure C-C stretching modes of the cation respectively, close to the strongest bands in the infrared spectrum⁷. All of the other strong features in the spectrum closely match the predicted a_g vibrational frequencies (or combinations thereof), as can be seen in Table 2.

Site Effects: Taking advantage of the narrow bandwidth of the laser, we tested the possibility that some of the emission structure might have arisen from site effects in the matrix. In particular, in unpublished work in this laboratory by *Joblin et al.*¹², spectral substructure observed on a 15-50 cm⁻¹ scale was closely examined. However, they were unable to discriminate between site effects and the possibility that this substructure was due to very low frequency modes peculiar to perylene (e.g. the “butterfly” and “accordion” modes (see *B. Fourmann et al.*^{13a}, *F. Fillaux*^{13b}, *S. Wittmeyer and M. Topp*^{13c} and *Joblin et al.*^{4b}). Here, using narrow band radiation, we excited the 730 nm absorption band every 3-5 nm from 720 to 750 nm, and measured the resulting spectrally resolved fluorescence from 960 nm to 790 nm, to observe whether any of the bands in this region could result from site effects due to the argon matrix (or Ar-complexes). Emission spectra at five selected excitation wavelengths (from the total of twelve spectra recorded in this experiment) are presented in Figure 4.

IV. DISCUSSION

The absorption spectrum of the perylene cation, presented in Figure 1, is consistent both in band positions and relative intensities with previous work^{4a,7}. Although the positions of the transitions corresponding to different electronic band systems closely matches those found by *Szczepanski et al.*⁷ (see Table 1), new calculations by *Hirata et al.*⁸ call for some reassignment. *Hirata et al.*⁸ have changed the ordering of the states previously identified as D₁, D₂ and D₃ by *Negri et al.*⁹ This new ordering seems to be entirely consistent with that observed experimentally by *Boschi et al.*⁶, and *Szczepanski et al.*⁷, as well as in this work. In particular, the lack of experimental observation of absorption into the state we now label as D₃ is entirely understood in terms of the symmetry of this state as ²B_{1u}, since an optical transition to this state is symmetry forbidden from the ground (²A_g) state.

Although the correspondence of our absorption spectrum to the qualitative relative intensities given by *Szczepanski et al.*⁷ is very good, the experimentally observed relative intensities do not reflect the relative oscillator strengths calculated by *Hirata et al.*⁸. They predict *f* values of 0.0001 and 0.0002 respectively for the transitions to D₁ and D₂, which are indeed observed to be weak. However, they calculate *f* to be 0.041 for the electronic transition to the D₄ state, which is clearly much weaker (in fact, it is barely visible if at all, in Fig. 1) than the transitions to D₁ and D₂. Their *f* value for the D₅ ← D₀ transition of 0.559 is consistent with the intense transition that we, along with *Szczepanski et al.*⁷, observe.

We note here the rather robust fluorescence that can be seen from the matrix-isolated perylene cation following laser excitation of typically a few millijoules per pulse. The gross vibrational structure in the fluorescence that is observed from the D₁ electronic state (see Figs. 2, 3 and 4) can almost entirely be assigned to totally symmetric vibrations, by comparison to the D₀ vibrational frequencies for perylene cation, calculated using density functional theory. This includes the relative importance of the pure C-C stretch and C-C stretch plus C-H in-plane bending combination already noted. This strongly suggests that the perylene cation largely maintains the D_{2h} symmetry of the parent molecule. In light of this, the fluorescence emission seems rather unremarkable.

However, we do note that the combination band $C_1^0 I_1^0$ would be expected to be more intense, based on the apparent Franck-Condon factors observed for C_1^0 and I_1^0 alone. Little evidence seems to exist for the participation of non-totally symmetric modes (which perhaps might be induced by interaction with the matrix) in the emission spectra.

It is quite apparent in comparing the emission resulting from pumping the D_2 vs D_3 states (Fig. 3), that rapid relaxation occurs to the D_1 electronic state before emission has a chance to occur. This relaxation must occur on a time scale much faster than the fluorescence lifetime, quite probably on the time scale of picoseconds or less. At this time, the exact mechanism of this relaxation process is not known. However, given that these molecules are trapped in a matrix, matrix interactions likely account, at least in part, for the rapid relaxation. Yet, in terms of the gross vibrational structure that is observed, we do not see evidence for matrix effects. Furthermore, the results displayed in Fig. 4 clearly argue against any major site effects being present in our Ar matrix. As the laser is tuned across the D_2 electronic state, the major features of the spectrum do not change, indicating that the perylene molecule occupies only one predominant site. Another important conclusion from this work is that the 15 -50 cm^{-1} fine substructure measured earlier in this laboratory^{4,12} reflects an inherent property of matrix-isolated perylene, and not a site effect. Taken together, these results seem a bit surprising, considering the propensity of argon to exhibit interactions with the guest molecule in the matrix due to its size and polarizability, and the well known property of aromatic molecules to form several complexes with Argon in the gas phase^{13c}.

However, examination of the global (overall) structure of the emission (and absorption) bands shows that several fluorescence bands are more intense with respect to the rest of the spectrum in argon but not in neon^{4a}. Interestingly, these are the bands which correspond to the most intense bands in the IR spectrum of the cation⁷ (identified here as H_1^0 , I_1^0 , and J_1^0). This suggests that the additional polarizability afforded by Ar over Ne significantly increases the Franck-Condon factors for just these vibronic bands which involve in-plane CC stretching vibrations, "borrowing" some of the intensity from the 0-0 band.

The emission that is seen from the perylene cation is interesting from an astrophysical standpoint because of the region in which it occurs. Visible emission features from UV excited objects in the galaxy thought to be associated with ionized PAHs fall in the red and near-infrared region, as do the bands reported here. These results support the hypothesis that PAH cations can contribute to the interstellar emission in the visible and near-IR, which is associated with carbon-rich objects. It is now required to check to see if a fluorescence signal can also be measured in the gas phase.

V CONCLUSION

The laser fluorescence spectra of the argon matrix isolated perylene cation ($D_1(^2B_{2g}) \rightarrow D_0(^2A_u)$), when the $D_2(^2B_{3g}) \leftarrow D_0(^2A_u)$ and $D_5(^2B_{3g}) \leftarrow D_0(^2A_u)$ transitions are excited, are presented, confirming the preliminary results of *Joblin et al*^{4a}. Strong evidence is presented that very fast, non-radiative relaxation occurs from D_5 or D_2 to D_1 , followed by radiative emission to D_0 . Tentative vibrational assignments have been made for the $D_1 \rightarrow D_0$ vibronic modes that are active in the spectrum. These compare favorably with the theoretically calculated values of the vibrational modes, with the strongest IR bands leading to the most intense vibronic bands. This behavior is not found in neon. It was found that the emission spectrum could be mostly explained based on activity of the totally symmetric vibrational modes which are expected to be active in the spectrum. An experiment in which the laser was tuned across the entire $D_2(^2B_{3g}) \leftarrow D_0(^2A_u)$ transition was performed demonstrating that the observed major transitions in the emission spectrum are not due to site effects, but are attributable to vibrational transitions within the $D_1(^2B_{2g}) \rightarrow D_0(^2A_u)$ manifold.

ACKNOWLEDGMENTS

This work was supported by NASA's Laboratory Astrophysics and Long-Term Space Astrophysics Programs. X.D.F.C thanks the *Swiss National Science Foundation* for his support. B.M.S acknowledges the *Stanford University/NASA Ames Research Center/American Association*

for Engineering Education (ASEE) Summer Faculty Fellowship Program for support. We would also like to acknowledge the excellent technical support of Mr. Robert Walker.

REFERENCES

- 1 a) L. J. Allamandola, D.M. Hudgins, and S.A. Sandford, *Astrophys. J. (Letters)* 511, L115 (1999).
- b) L.J. Allamandola A.G.G.M. Tielens, and J.R. Barker, *Astrophys.J. Suppl. Ser.* 71, 733 (1989).
- c) J. L. Puget and A. Leger, *Ann. Rev. Astron. Astrophys.* 27,161 (1989).
- 2 a)G.P. van der Zwet, and L.J. Allamandola, *Astron. Astrophys.* 146, 76 (1985).
- b) M.K. Crawford, A.G.G.M. Tielens and L.J. Allamandola, *Astrophys. J. Letters* 293, L45, (1985).
- c) A. Leger, and L.B. d'Hendecourt, *Astron. and Astrophys.* 146, 81, (1985).
- d) F. Salama, and L.J. Allamandola, *J. Chem. Soc. Faraday Trans.* 89, 2277 (1993).
- e)F. Salama, E. Bakes, L.J. Allamandola, and A.G.G.M. Tielens, *Astrophys. J.* 458, 621 (1996).
- f) F. Salama, G.A. Galazutdinov, J. Krelowski, L.J. Allamandola, and F.A. Musaev, *Astrophys. J.* 526, 265 (1999).
- 3a S.M. Scarrott, S. Watkin, J.R. Miles, and P. J. Sarre, *Mon. Not. Roy. Astro. Soc.*, 255, 1P (1992).
- b G.D. Schmidt, M. Cohen ,and B. Margon, *Astrophys. J. Lett.* 239, L133 (1980)
- c N. K. Rao,, and D.L. Lambert, *Mon. Not. Roy. Astro. Soc.*, 263, L27 (1993)
- 4 a) C. Joblin, F. Salama, and L.J. Allamandola, *J. Chem. Phys. (Lett)* 102, 9743 (1995).
- b) C. Joblin, F. Salama, and L.J. Allamandola, *J. Chem. Phys.* 110, 7287 (1999).
- 5 X.D.F. Chillier, B.M. Stone, B.M., F. Salama, and L.J. Allamandola, *J. Chem. Phys. (Lett.)* 111, 449, (1999)
- 6 R. Boschi, J.N. Murrell, W. and Schmidt, *Discussions Faraday Soc.* 54, 116, (1972).
- 7) J. Szczepanski, C. Chapo, and M. Vala, *Chem. Phys. Lett.*, 205, 434, (1993)
- 8) S. Hirata, T. J.Lee, and M. Head-Gordon, *J. Chem. Phys.*, xxx, xx, (???)
- 9) F. Negri,, and M. Z. Zgierski, *J. Chem. Phys.*, 100, 1387, (1994).

10) S. Langhoff, unpublished results.

11) S. Leach, in *Polycyclic Aromatic Hydrocarbons and Astrophysics*, edited by . A. Leger, L. B. d'Hendecourt, and N. Boccarda, [D.Reidel, Dordrecht) 99, (1987].

12) C. Joblin, F. Salama, and L.J. Allamandola, unpublished results.

13)a B. Fourmann, C. Jouvot, A. Tramer, J. M. LeBars, and Ph. Millie *Chem. Phys.*, 92, 25, (1985).

b) F. Fillaux, *Chem. Phys. Lett.*, 114, 3847, (1985).

c) S. A. Wittmeyer, and M. R. Topp, *J. Phys. Chem.*, 1993, 8718, (1993).

Table Captions:

Table 1: Perylene cation electronic state transition energies in e.v. from D_0 (ground state). Previous experimental and theoretical values are presented, along with results reported here. Calculated oscillator strengths, when available, are also given.

Table 2: Perylene cation $D_1 \rightarrow D_0$ fluorescence: major features and assignments. Peak positions of major vibrational features are given in cm^{-1} , along with the displacement from the electronic origin, and a designation for assignment purposes. Assignments, in terms of theoretical values of vibrational frequencies of a_g symmetry, are suggested.

Table 1. Perylene cation electronic state transition energies in e.v. from D₀ (ground state).

State		THEORY ^a		EXPERIMENT ^b		
State	Symmetry	QCFF/PI ^c	TDDFT ^d	PES ^e	Ar matrix ^f	This work
D ₁	² B _{2g}	1.84 (0.0006)	1.62-1.65 (0.0001)	1.55 [800] ^b	1.56 [791] vw	1.57 [790] w
D ₂	² B _{3g}	1.60 (0.0511)	1.68-1.73 (0.0002)	1.68 [738]	1.69 [734] m	1.69 [733] m
D ₃	² B _{1u}	1.79 (0.0000)	1.77-1.80 (forbidden)	-	-	-
D ₄	² B _{2g}	1.90 (0.0025)	1.90-2.01 (0.041)	1.90 [653]	1.93 w [643]	1.94 [640] vw
D ₅	² B _{3g}	2.47 (0.5679)	2.43-2.72 (0.559)	2.34 [530]	2.32 s [534]	2.32 [535] s
D ₆	² B _{2g}	(0.0000)	-	3.4	3.73	
D ₇	-	(0.0000)	-	-	4.04	

a. calculated oscillator strengths are given in parentheses

b. wavelength in nanometers (measured) are given in brackets, relative band strengths listed as s, m, w, vw; indicate absorptions which are strong, moderate, weak, very weak.

c. QCFF/PI+CI calculations from Ref. 9

d. TDDFT and TDDFT/TDA calculations from Ref. 8

e. Photoelectron spectroscopy from Ref. 6

f. Matrix isolation spectroscopy from Ref. 7

Table 2. Perylene cation $D_1 \rightarrow D_0$ fluorescence: major features and assignments.

Peak Position $\nu(\text{cm}^{-1})$	Designation ^a	$\Delta\nu$ $\nu(\text{cm}^{-1})$	Assignment $\nu(\text{cm}^{-1})$	S_0 a _g Vibration $\nu(\text{cm}^{-1})$ ^b
12623	0-0	0	0	-
12506	A	117	-	-
12420	B	203	-	-
12266	C_{10}^0	357	0-357	351.1
12189	D_{10}^0	434	0-434	467.5
12091	E_{10}^0	532	0-532	540.1
11900	C_{20}^0	723	0-2x357	-
11727	$C_1^0 E_{10}^0$	896	0-(357+532)	-
11685	$C_2^0 B$	938	0-(203+2x357)	-
11654	F_{10}^0	969	0-969	981.6
11400	G_{10}^0	1223	0-1223	1214.0
11325	H_{10}^0	1298	0-1298	1299.0
11236	I_{10}^b	1387	0-1387	1365.6
11026	J_{10}^0	1597	0-1597	1565.1
10875	$C_1^b I_{10}^0$	1748	0-(1387+357)	-
10780	$D_{10}^0 I_{10}^0$	1843	0-(434+1387)	-
10680	$C_1^0 J_{10}^0$	1943	0-(1597+357)	-
	F_2^0		0-(2x969)	

a. See Fig.2

b. Langhoff, unpublished results.

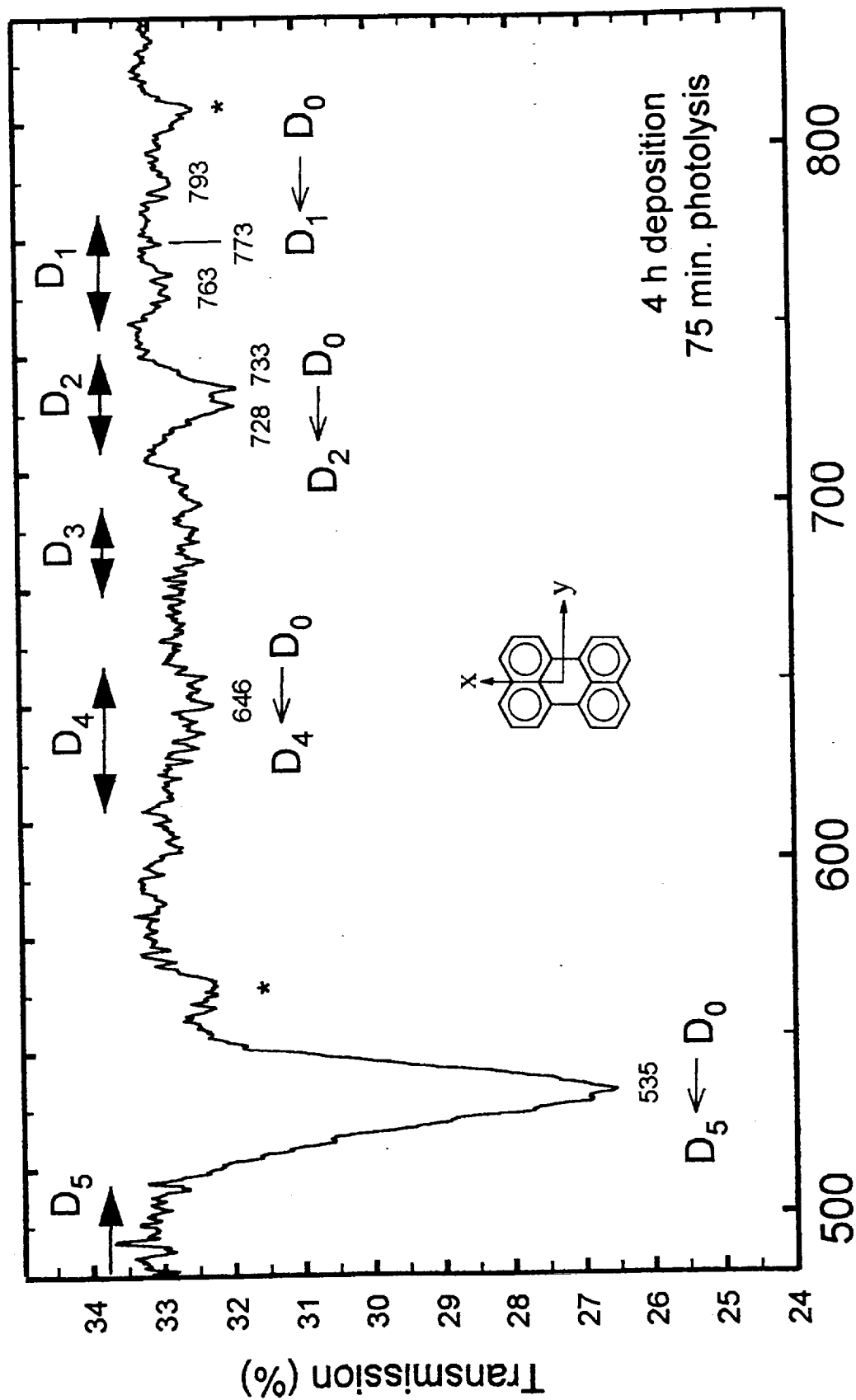
Figure Captions:

Figure 1: Visible/near-infrared absorption spectrum of the perylene cation isolated in an argon matrix at 10K after 4 hours of deposition followed by 75 minutes of photolysis. Regions in which electronic transitions are expected to occur, based on theoretically determined energies for the excited electronic states (see Table 1 and Ref. 8) are indicated by double-headed arrows at the top. Our assignments of the absorption features, due to electronic transitions from D_0 to the D_1 , D_2 , D_4 and D_5 states, are indicated. The axis system of the perylene molecule used to assign the state symmetries listed in Table 1 is also shown. The bands marked with an asterisk (*) near 560 and 810 nm are due to the counterion (the perylene anion; Halasinski, unpublished results).

Figure 2: A comparison of the dispersed fluorescence from the perylene cation isolated in an argon matrix, following laser excitation of the $D_5(^2B_{3g}) \leftarrow D_0(^2A_u)$ transition at 535 nm and the $D_2(^2B_{3g}) \leftarrow D_0(^2A_u)$ transition at 731.2 nm, demonstrating that emission occurs in both cases from the D_1 state. Asterisks indicate artifacts due to the scattering of laser light from the grating.

Figure 3: Dispersed fluorescence from the perylene cation isolated in an argon matrix, resulting from laser excitation of the $D_2(^2B_{3g}) \leftarrow D_0(^2A_u)$ transition at 731.2 nm. Designations are made for the major vibrational features, according to the assignments given in Table 2.

Figure 4: Dispersed fluorescence following the laser excitation of the $D_2(^2B_{3g}) \leftarrow D_0(^2A_u)$ transition of the perylene cation isolated in an argon matrix, as the laser is tuned across the electronic band. Asterisks indicate artifacts produced by the scattering of laser light from the grating.



Wavelength (nm)

Wavelength (nm)

940 920 900 880 860 840 820 800

Arbitrary Units

$\lambda_{\text{exc}} = 731 \text{ nm}$

*

*

$\lambda_{\text{exc}} = 535 \text{ nm}$

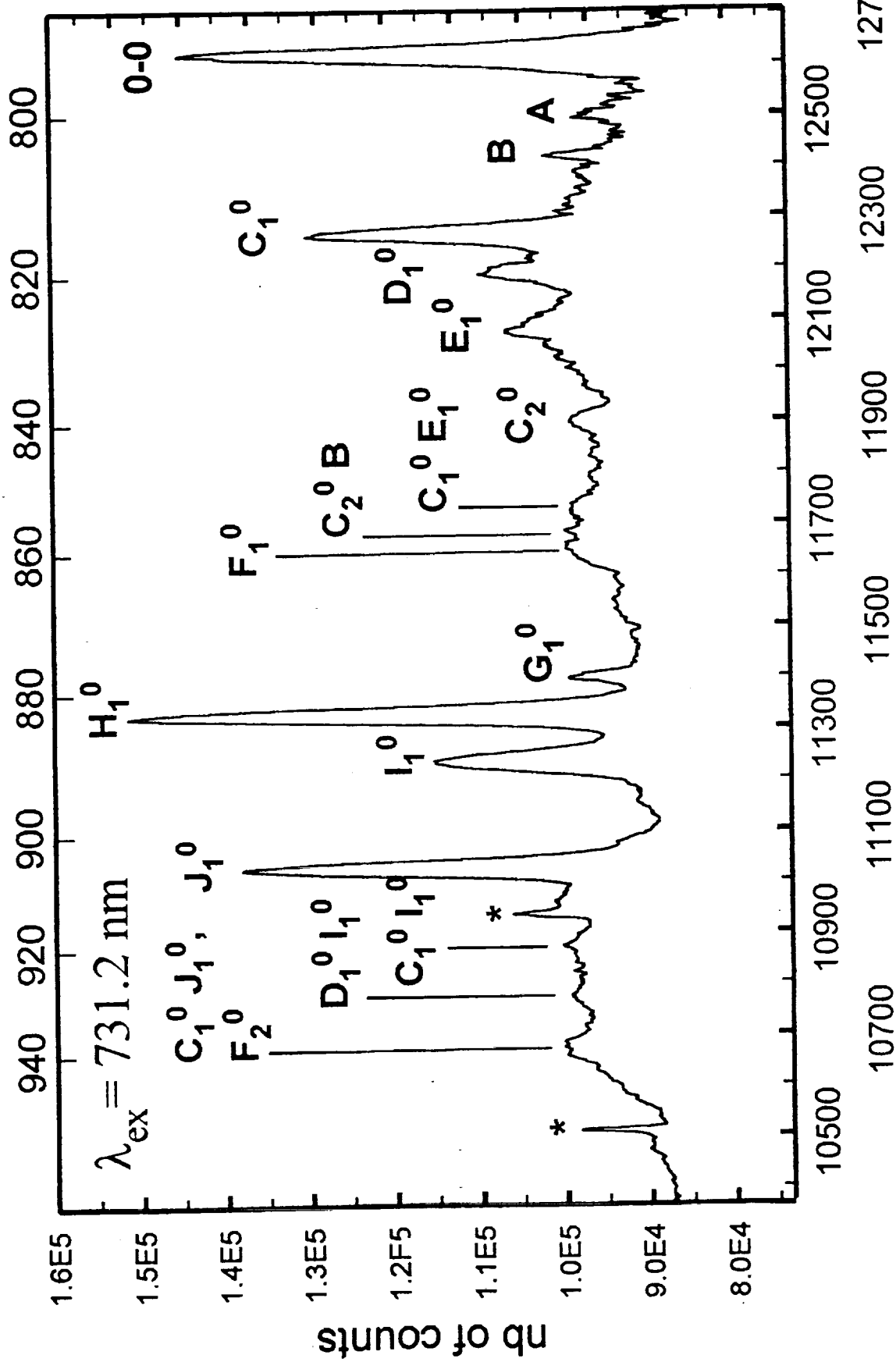
*

10500 10900 11300 11700 12100 12500

10700 11100 11500 11900 12300 12700

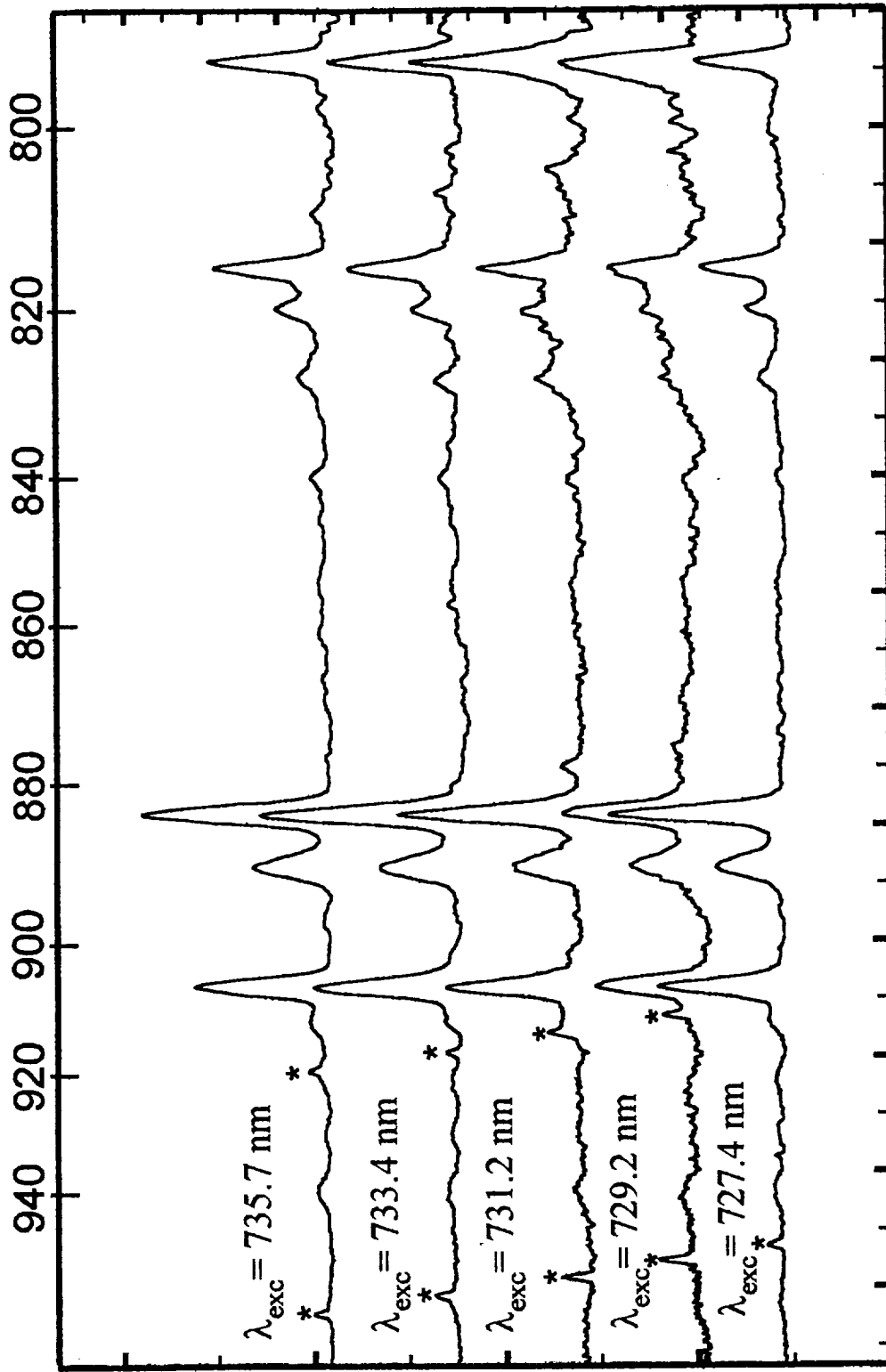
Wavenumber (cm^{-1})

Wavelength (nm)



Wavenumber (cm^{-1})

Wavelength (nm)



10500 10700 10900 11100 11300 11500 11700 11900 12100 12300 12500 12700

Wavenumber (cm^{-1})